PAPER

Enhancing the output current of a CdTe solar cell *via* a CN-free hydrocarbon luminescent down-shifting fluorophore with intramolecular energy transfer and restricted internal rotation characteristics†

Yilin Li,‡[a] Joseph Olsen‡[a] and Wen-Ji Dong*[a,b]

A CN-free hydrocarbon fluorophore (**Perylene-TPE**) was synthesized as a new luminescent down-shifting (LDS) material. Its photophysical properties in both the solution state and the solid state were studied. The unity fluorescence quantum yield of **Perylene-TPE** observed in its solid state is considered to be from the characteristics of intramolecular energy transfer (IET) and restricted internal rotation (RIR). This is supported by the results from theoretical calculations and spectroscopic measurements. For the photovoltaic application of **Perylene-TPE**, a theoretical modeling study suggests that using the LDS film of **Perylene-TPE** may increase the output short circuit current density (J_{sc}) of a CdTe solar cell by 2.95%, enhance the spectral response of a CdTe solar cell at 400 nm by 41%, and shift the incident solar photon distribution from short-wavelength (<500 nm) to long-wavelength (>500 nm). Experimentally, placing a LDS film of **Perylene-TPE** on a CdTe solar cell can enhance its output J_{sc} by as high as 3.30 ± 0.31%, which is comparable to the current commercially available LDS material – Y083 (3.28% ± 0.37%).

Introduction

Luminescent down-shifting (LDS) is one of the solar spectral shaping methods that modify the incident solar photon distribution to match the maximum spectral response region of a solar cell.[1–3] Till now, a variety of luminescent species such as quantum dots,[4,5] organic fluorophores[6,7] and rare-earth complexes[8,9] has been used as LDS materials to enhance the spectral response of the solar cell at short-wavelength. Among these LDS materials, organic fluorophores have been the most attractive because their photophysical properties can be fine-tuned by their chemical structures. Ideal organic fluorophores for LDS application require specific photophysical properties including both high fluorescence quantum yield and large Stokes shift in the solid state.[10] However, early studies showed that the fluorescence quantum yield and Stokes shift compromise each other, *i.e.* increasing the value of one will decrease the value of the other.[11,12] Therefore, although a large number of organic fluorophores has been tried for LDS application, few of them result in the performance improvement of the solar cell.[13–15]

Structurally modified perylene derivatives from commercial sources (BASF Lumogen F dyes) such as Y083, Y170, O240 and R300 were first used as LDS materials to enhance the output short circuit current density (J_{sc}) of the CdTe solar cell or CIGS solar cell.[16–19] Recently, several tetraphenylethylene (TPE)-based organic fluorophores with both intramolecular charge transfer (ICT) and aggregation-induced emission (AIE) characteristics have been synthesized as LDS materials for the CdTe solar cell.[20] Although as high as 3–6% of J_{sc} enhancement on the latest CdTe cells was achieved by using these perylene (or TPE)-based organic LDS materials, the potential environmental impact of these organic LDS materials has not been evaluated. It has been noted that cyano (CN) groups were introduced into the chemical structures of these organic fluorophores (*e.g.* Y083 and Y170) to improve their photophysical properties for LDS application. Thereby, toxic materials (CuCN, malononitrile or other CN-containing chemicals) were inevitably used during the synthesis of these organic fluorophores. Furthermore, the photo-degradation of such

[a]*Voiland School of Chemical Engineering and Bioengineering, Washington State University, Pullman, WA 99164, USA. E-mail: wdong@vetmed.wsu.edu*
[b]*Department of Integrative Physiology and Neuroscience, Washington State University, Pullman, WA 99164, USA*

†Electronic supplementary information (ESI) available: Fig. S1–S4 and Tables S1–S2. NMR and MS of synthesized compounds. Theoretical calculation results of the optimal geometry of **Perylene-TPE** at ground state. See DOI: 10.1039/c4pp00480a

‡These authors contributed equally.

This journal is © The Royal Society of Chemistry and Owner Societies 2015

Photochem. Photobiol. Sci., 2015, **14**, 833–841 | 833

CN-containing organic fluorophores may release toxic CN-containing gases, which are hazardous to the environment.[21,22]

To address the potential environmental issue of current LDS materials, we proposed a CN-free hydrocarbon fluorophore in this paper. Hydrocarbon materials are well known to have less environmental impact because only carbon and hydrogen are contained in the molecular structures and thus, combusting these hydrocarbon materials releases only CO_2 and H_2O. In this report, we studied the photophysical properties of this newly synthesized CN-free hydrocarbon fluorophore and investigated its LDS applications on a CdTe solar cell both theoretically and experimentally.

Results and discussion

Molecular synthesis

The molecular structure of **Perylene-TPE** and its synthetic method are depicted in Scheme 1. The molecular structure of **Perylene-TPE** consists of two critical building blocks of current LDS materials – perylene and tetraphenylethylene (TPE). The strategy for synthesizing **Perylene-TPE** is to couple **Perylene-Bpin** with **TPE-Br**. **Perylene-Bpin** was synthesized by the bromination of **Perylene** to get **Perylene-Br**, followed by the reaction with B_2pin_2. **TPE-Br** was synthesized from the reaction of **DPM** and 4-bromobenzophenone, followed by the dehydration of **TPEol-Br**. This synthetic route avoids using any CN-containing chemicals and therefore, the structure of **Perylene-TPE** is totally CN free. In the structure of **Perylene-TPE**, both the perylene group and the TPE group are reported to have minimal or no impacts on the environment or human beings, so it is reasonable to consider **Perylene-TPE** as an environmentally friendly compound.[23,24] Although potentially hazardous organic solvents such as DMF, 1,4-dioxane, THF and toluene were used during the synthesis of **Perylene-TPE**, most of the solvents can be recycled in the lab or replaced by other environmentally friendly solvents in the industry.[25]

Reaction (i): 3-bromoperylene (Perylene-Br). To a solution of **Perylene** (1.0 g, 4.0 mmol) in 100 mL of DMF was added a solution of *N*-bromosuccinimide (NBS, 705 mg, 4.0 mmol) in 50 mL of DMF dropwise. The resulting solution was stirred at room temperature for 16 h. The solvent was evaporated. Recrystallization from toluene affords the product (yellow solid, 1.0 g, isolated yield 77%). ¹H-NMR (300 MHz, CDCl₃, δ): 8.23–8.06 (m, 4H), 7.98 (d, 1H, J = 8.1 Hz), 7.76–7.69 (m, 3H), 7.60–7.44 (m, 3H). The characterization data are consistent with the reported literature.[26]

Reaction (ii): 4,4,5,5-tetramethyl-2-(perylen-3-yl)-1,3,2-dioxaborolane (Perylene-Bpin). **Perylene-Br** (500 mg, 1.5 mmol), B_2pin_2 (767 mg, 3.0 mmol), Pd(dppf)Cl₂ (33 mg, 3 mol%) and KOAc (444 mg, 4.5 mmol) were dissolved in 50 mL of 1,4-dioxane. The reaction mixture was heated to 100 °C for 16 h. The solvent was extracted with DCM twice and the combined organic layers were dried over anhydrous MgSO₄. The solvent was evaporated and the residue was purified by silica gel chromatography using Hex–EtOAc (30 : 1) as an eluent to afford the product (yellow solid, 252 mg, isolated yield 44%). ¹H-NMR (300 MHz, CDCl₃, δ): 8.68 (dd, 1H, J = 8.4 Hz), 8.24–8.16 (m, 4H), 8.08 (d, 1H, J = 7.6 Hz), 7.71 (t, 2H), 7.57–7.44 (m, 3H), 1.45 (s, 12H). MALDI-MS: *m*/*z* calcd for $C_{26}H_{24}BO_2^+$ 379.1869, found 379.2639. The characterization data are consistent with the reported literature.[27]

Reaction (iii): 1-(4-bromophenyl)-1,2,2-triphenylethanol (TPEol-Br). To a solution of **DPM** (2.0 g, 11.9 mmol) in 20 mL of anhydrous THF was added a 1.6 M solution of *n*-BuLi in hexanes (7.4 mL, 11.9 mmol) at 0 °C under a nitrogen atmosphere. The resulting solution was stirred for 30 min at that temperature. To this solution was added 4-bromobenzophenone (3.1 g, 11.9 mmol) and the reaction mixture was allowed to warm to room temperature with stirring for a 6 h period. The reaction was quenched with the addition of water, the organic layer was extracted with DCM twice and the combined organic layers were dried over anhydrous MgSO₄. The solvent was evaporated to afford the crude product (white solid, 2.6 g).

Reaction (iv): (2-(4-bromophenyl)ethene-1,1,2-triyl)tribenzene (TPE-Br). The crude **TPEol-Br** (2.6 g, 6.1 mmol) and a catalytic amount of *p*-toluenesulphonic acid monohydrate (*p*-TsOH·H₂O, 500 mg, 2.6 mmol) were added to 80 mL of
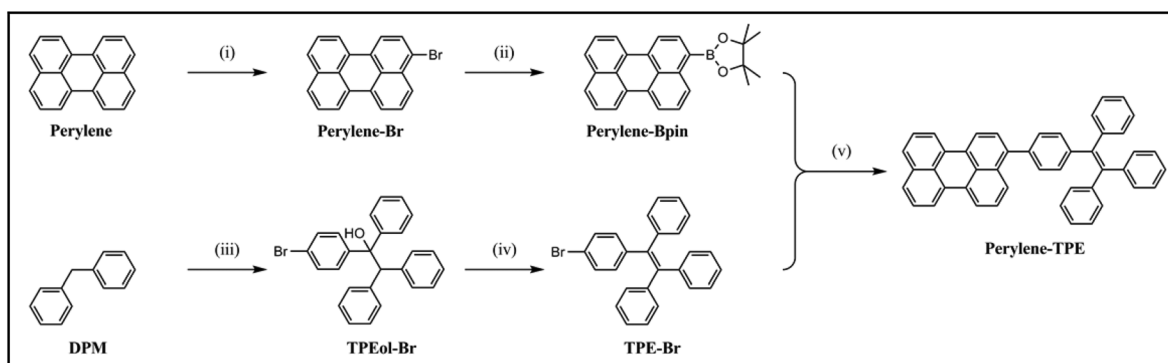
Scheme 1 Molecular structure and synthetic route of **Perylene-TPE**. Reaction reagents and conditions: (i) NBS, DMF, rt, 16 h; (ii) B₂pin₂, Pd(dppf)Cl₂, KOAc, 1,4-dioxane, 100 °C, 16 h; (iii) a. *n*-BuLi, THF, 0 °C, N₂, 30 min, b. 4-bromobenzophenone, rt, N₂, 6 h; (iv) *p*-TsOH·H₂O, toluene, reflux, 16 h; (v) Pd(PPh₃)₄, K₂CO₃ (aq.), EtOH, toluene, reflux, 16 h.

toluene in a 150 mL flask equipped with a Dean–Stark trap. The resulting solution was heated to reflux for 16 h. The reaction mixture was extracted with DCM twice and the combined organic layers were dried over anhydrous $MgSO_4$. The solvent was evaporated and the residue was purified by silica gel chromatography using Hex as an eluent to afford the product (white solid, 2.0 g, isolated yield 80%). ^{1}H-NMR (300 MHz, $CDCl_3$, δ): 7.31 (d, 2H, J = 8.5 Hz), 7.22–7.11 (m, 15H), 7.01 (d, 2H, J = 8.6 Hz). ^{13}C-NMR (75 MHz, $CDCl_3$, δ): 143.8, 143.7, 143.6, 143.0, 141.9, 140.0, 133.4, 131.7, 131.6, 131.6, 131.2, 128.2, 128.1, 128.0, 127.1, 127.0, 127.0, 120.8. MALDI-MS: m/z calcd for $C_{26}H_{19}Br^+$ 410.0670, found 410.0552. The characterization data are consistent with the reported literature.[28]

Reaction (v): 3-(4-(1,2,2-triphenylvinyl)phenyl)perylene (Perylene-TPE). **Perylene-Bpin** (200 mg, 0.53 mmol), **TPE-Br** (261 mg, 0.63 mmol), Pd(PPh₃)₄ (31 mg, 5 mol%) and K_2CO_3 (110 mg, 0.79 mmol, dissolved in 1 mL of water) were added into a mixture of 1 mL of EtOH and 25 mL of toluene. The reaction mixture was heated to reflux for 16 h. After cooling down, the reaction mixture was extracted by DCM. The organic phase was collected and dried over anhydrous $MgSO_4$. The solvent was removed and the residue was purified by silica gel chromatography using Hex–DCM (2 : 1) as the eluent to afford the product (yellow solid, 200 mg, isolated yield 65%). ^{1}H-NMR (300 MHz, $CDCl_3$, δ): 8.20 (d, 2H, J = 7.8 Hz), 7.73–7.67 (m, 2H), 7.51–7.39 (m, 2H), 7.34–7.26 (m, 3H), 7.19–7.05 (m, 21H). ^{13}C-NMR (75 MHz, $CDCl_3$, δ): 144.0, 144.0, 144.0, 144.0, 143.9, 143.9, 143.1, 143.0, 141.6, 141.3, 140.9, 140.8, 140.0, 138.9, 138.5, 134.9, 133.1, 132.0, 131.7, 131.7, 131.6, 131.6, 130.7, 129.5, 129.3, 128.9, 128.0, 128.0, 127.9, 127.9, 126.9, 126.8, 126.7, 126.7, 126.3, 126.1, 120.6, 120.5, 120.3, 120.1. MALDI-MS: m/z calcd for $C_{46}H_{30}^+$ 582.2348, found 582.2097.

Photophysical studies

Photophysical properties of **Perylene-TPE** were studied using spectroscopic measurements of absorption and emission spectra, fluorescence quantum yields and fluorescence lifetime in the solution state and the solid state. Solution samples were prepared by dissolving **Perylene-TPE** in THF. Solid samples were prepared by doping **Perylene-TPE** into PMMA thin films (or LDS films). The preparation method of the solid samples is the same as that of the LDS films, which is described in the Experimental section. Low concentrations of **Perylene-TPE** were used in both solution (15 μM) and solid (<2.0%, w/w) samples to minimize the optical re-absorption problem. The experimental conditions are described in the Experimental section. The absorption and emission spectra of the solution and solid samples of **Perylene-TPE** are depicted in Fig. 1. The pertinent photophysical parameters are summarized in Table 1.

For the THF solution samples (blue lines) of **Perylene-TPE** in Fig. 1, the absorption spectrum of **Perylene-TPE** exhibits two major peaks at 330 nm and 448 nm. The peak at 330 nm can be ascribed to the TPE group in its molecular structure because TPE exhibits maximal absorption at 310 nm (Fig. S1†).
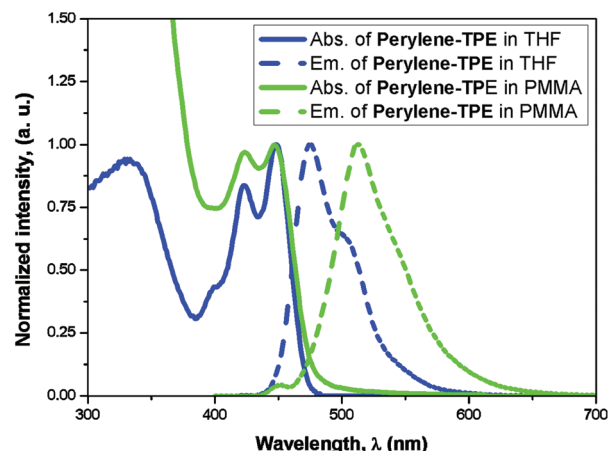

Fig. 1 Absorption (solid line) and emission (dashed line) spectra of **Perylene-TPE** in THF solution (blue) and PMMA solid film (green).

The emission spectrum of **Perylene-TPE** exhibits the pattern of mirror image to its absorption spectrum, which is similar to perylene (Fig. S2†). This suggests that the perylene group in the **Perylene-TPE** molecule dominates the electron transitions of the molecule during its absorption and emission processes, leading to the observed π–π* electron transition of **Perylene-TPE**. Compared to perylene (λ_{abs} = 437 nm, λ_{em} = 446 nm and $\Delta\lambda$ = 9 nm, in Fig. S2†), the absorption and emission maxima (λ_{abs} = 448 nm, λ_{em} = 474 nm, in Table 1) of **Perylene-TPE** are red-shifted with a larger Stokes shift ($\Delta\lambda$ = 26 nm, in Table 1). This is because the π-conjugation size of **Perylene-TPE** is larger than that of perylene, which lowers the overall molecular energy and shifts the absorption and emission spectra to longer wavelengths. A lower fluorescence quantum yield and shorter fluorescence lifetime (Φ_f = 0.56 and τ_f = 1.41 ns, in Table 1) of **Perylene-TPE** than those of **Perylene** (Φ_f = 1.00 and τ_f = 4.10 ns, in Fig. S2†) indicate that the attachment of TPE to perylene leads to an increase in the non-radiative decay rate constant (k_{nr}) of the molecule (k_{nr} from 0 to 0.31 ns^{-1}, in

Table 1 Photophysical parameters including absorption wavelength (λ_{abs}), molar absorption coefficient (ε), emission wavelength (λ_{em}), Stokes shift ($\Delta\lambda = \lambda_{em} - \lambda_{ebs}$), fluorescence quantum yield (Φ_f), fluorescence lifetime (τ_f), radiative ($k_r = \Phi_f/\tau_f$) and non-radiative ($k_{nr} = (1 - \Phi_f)/\tau_f$) decay rate constants of **Perylene-TPE** in THF solution and PMMA solid film

	THF solution	PMMA solid film[a]
λ_{abs} (nm)	448	448
ε (M^{-1} cm^{-1})	40 866	10 360
λ_{em} (nm)	474	512
$\Delta\lambda$ (nm)	26	64
Φ_f[b]	0.56	1.00[c]/1.00[d]
τ_f (ns)	1.41	2.88
k_r (ns^{-1})	0.40	0.35
k_{nr} (ns^{-1})	0.31	0

[a] Fluorophore weight concentration is 1.0%; film thickness is 50 μm. [b] For solution samples, 4-dimethylamino-4′-nitrostilbene (Φ_f = 0.53 in benzene) was used as a standard;[29] for solid samples, an integrating sphere was used.[30] [c] Excited at 474 nm. [d] Excited at 330 nm.

This journal is © The Royal Society of Chemistry and Owner Societies 2015

Photochem. Photobiol. Sci., 2015, **14**, 833–841 | 835

Fig. S2† and Table 1). The high k_{nr} is believed to be from the σ-bond rotation of the TPE group in **Perylene-TPE** that promotes the excited electron going through non-radiative decay pathways.

For the PMMA solid samples (green lines) of **Perylene-TPE** in Fig. 1, it is noted that the absorption spectrum of **Perylene-TPE** in its solid state exhibits the same absorption wavelength as its solution state. This observation can be explained by the Franck–Condon principle that the photon absorption process occurs very rapidly, in femtoseconds, which makes the absorption spectrum of **Perylene-TPE** environmentally independent. However, the emission spectrum of **Perylene-TPE** exhibits a red-shift by 38 nm in its solid state, which is different from that observed in its solution state. The disappearance of the mirror image pattern of the absorption spectrum is because the emission of **Perylene-TPE** starts from a non-equilibrium excited state, at which the random molecular orientation and conformational disorder of **Perylene-TPE** are inhibited in the PMMA solid film.[31] It is also noted that **Perylene-TPE** exhibits higher fluorescence quantum yield ($\Phi_f = 1.00$, in Table 1) with longer fluorescence lifetime ($\tau_f = 2.88$ ns, in Table 1) in its solid state than in its solution state. This unique spectroscopic feature of **Perylene-TPE** can be attributed to the intramolecular energy transfer (IET) and restricted internal rotation (RIR) characteristics of **Perylene-TPE**. For the IET characteristic, it has been reported that TPE only exhibits 0.50 of fluorescence quantum yield in its solid state while perylene exhibits unity.[32] Therefore, the near unity fluorescence quantum yield of **Perylene-TPE** when excited at 330 nm is most likely caused by the IET process in the **Perylene-TPE**, in which the absorbed energy by the TPE group efficiently transfers to the perylene group. For the RIR characteristic, it has been reported that most of the TPE-based fluorophores have a longer fluorescence lifetime in the solid state than in their solution state.[33,34] This is because the σ-bond rotation is restricted in the solid state, which significantly impedes the non-radiative decay rate.

To further understand the IET and RIR characteristics of **Perylene-TPE**, we performed theoretical calculations and spectroscopic measurements. First, the IET characteristic of **Perylene-TPE** was investigated by quantum chemical calculations. The highest occupied molecular orbital (HOMO) and the lowest unoccupied molecular orbital (LUMO) as well as the corresponding energy of TPE, perylene and **Perylene-TPE** were calculated by the DFT method based on their optimal geometries at the ground state. The results are depicted in Fig. 2.

It is noted in Fig. 2 that calculations of the compound – TPE, perylene and **Perylene-TPE** all show π–π* electron transition, which is consistent with the observations from the absorption spectra of TPE (Fig. S1†), perylene (Fig. S2†) and **Perylene-TPE** (Fig. 1). The calculated energies of HOMO and LUMO of perylene (−4.953 eV and −1.892 eV) are between that of TPE (−5.318 eV and −1.203 eV), which promotes the IET from TPE to perylene when they are conjugated. Moreover, the calculated HOMO and LUMO of **Perylene-TPE** suggest that the MOs are primarily located on its perylene group, which supports our previous discussion that its perylene group dominates the electron transition of **Perylene-TPE**. Further analyses
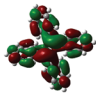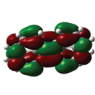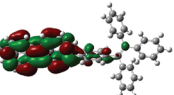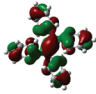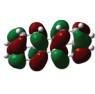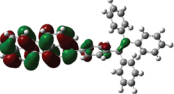

MO	TPE	perylene	**Perylene-TPE**
LUMO	−1.203 eV	−1.892 eV	−1.917 eV
HOMO	−5.318 eV	−4.953 eV	−4.864 eV

Fig. 2 HOMO and LUMO as well as the corresponding energy of TPE, perylene and **Perylene-TPE**.

on charge distribution show that its perylene group possesses 89% and 92% of the whole charge in **Perylene-TPE** on HOMO and LUMO, respectively (Table S1†). This means that 3% (= 92% − 89%) of the charge flows from its TPE group to its perylene group when **Perylene-TPE** is excited. Such charge flow strongly supports the IET characteristic of **Perylene-TPE**.

Then, the RIR characteristic of the **Perylene-TPE** in its solid state is examined by measuring the fluorescence quantum yields in water–acetonitrile mixtures with various water fractions (f_w, v/v%). This experiment is designed based on the fact that **Perylene-TPE** is hydrophobic, which is a common property of hydrocarbons. Therefore, adding water in its acetonitrile solution will cause the aggregation of the **Perylene-TPE**. In the aggregated state of **Perylene-TPE**, the σ-bond rotation of its TPE group is restricted, thus, **Perylene-TPE** will exhibit RIR characteristics. Moreover, the TPE group of **Perylene-TPE** prevents potential π–π* stacking of the molecules in the solid state – a known mechanism of fluorescence quenching in aggregated samples.[31] Therefore, a strong emission of **Perylene-TPE** in its aggregated form is expected. The experimental results are depicted in Fig. 3.

It is noted in Fig. 3 that **Perylene-TPE** exhibits two phases in the change of its fluorescence quantum yield with the
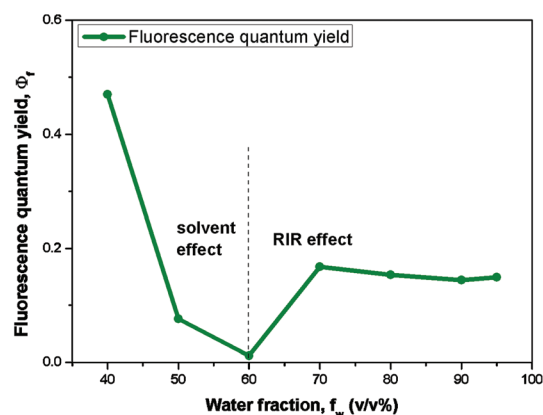

Fig. 3 Change of fluorescence quantum yields of **Perylene-TPE** in solvent mixtures with various water fractions from 40% to 95%. Fluorophore concentration is 15 μM.

836 | *Photochem. Photobiol. Sci.*, 2015, **14**, 833–841

This journal is © The Royal Society of Chemistry and Owner Societies 2015

increase of water fraction from 40% to 95%. At low water fraction (f_w < 60%), its fluorescence quantum yield decreases when increasing f_w. This is because increasing the water fraction in the solvent mixture leads to the increase in solvent polarity and the fluorescence solvent effect dominates the emission process of **Perylene-TPE**.[35,36] Further increasing the water fraction (f_w > 60%) will cause the aggregation of the **Perylene-TPE**. Its internal σ-bond rotation is gradually restricted, and thus the non-radiative decay rate decreases. Also, its TPE group prevents the perylene group from π–π stacking. The RIR characteristic of **Perylene-TPE** leads to the increase in its fluorescence quantum yield. Moreover, compared to the solid state of **Perylene-TPE** in PMMA solid films, its aggregated state exhibits a more red-shifted emission centered at 542 nm (Fig. S3†). In the PMMA solid film, the internal rotation of **Perylene-TPE** is restricted by the surrounding PMMA molecules while in its aggregated state, the internal rotation is restricted by itself, which introduces intermolecular interactions that shift the emission of **Perylene-TPE** to a longer wavelength.

Photovoltaic application

It is noted in Fig. 1 that the absorption of **Perylene-TPE** in the PMMA solid sample is below 500 nm, while its emission is over 500 nm, which suggests that **Perylene-TPE** is a suitable candidate as an LDS material for CdTe solar cell application. The LDS capability of **Perylene-TPE** was first investigated theoretically by a simple LDS model. The theoretical predictions include the effects of the LDS films with various **Perylene-TPE** concentrations (w/w%) on short circuit current density (J_{sc}) and external quantum efficiency (EQE) of a CdTe solar cell as well as incident photon distribution (ϕ) on the cell surface. The related equations are:

$$J_{LDS}\% = \frac{J_{sc+LDS} - J_{sc}}{J_{sc}} = J_{gain}\% - J_{loss}\%$$
$$= \frac{F_{abs} \times F_{em} \times F_{pc}}{F_{cell}} - J_{loss}\% \quad (1)$$

$$EQE_{LDS}(\lambda) = EQE(\lambda)T(\lambda) + F_{em} \times F_{pc} \times [1 - T(\lambda)] \quad (2)$$

$$\phi_{LDS}(\lambda) = T(\lambda)\phi(\lambda) + F_{abs} \times F_{pc} \times \frac{Em(\lambda)}{\int Em(\lambda)d\lambda} \times \int \phi(\lambda)d\lambda \quad (3)$$

Eqn (1) calculates the percentage of cell J_{sc} increase ($J_{LDS}\%$), which can be considered as the difference between the J_{sc} increase percentage ($J_{gain}\%$) and J_{sc} decrease percentage ($J_{loss}\%$) due to the LDS film. $J_{gain}\%$ in eqn (1) can be further expressed by several factors including absorption spectral matching factor (F_{abs}), emission spectral match factor (F_{em}), photon conversion and collection efficiencies factor (F_{pc}) and cell factor (F_{cell}). The detailed expressions of these factors are described in the Experimental section. Eqn (2) calculates the modified cell EQE ($EQE_{LDS}(\lambda)$), where $EQE(\lambda)$ is the cell EQE without the LDS film and $T(\lambda)$ is the transmission spectrum of the LDS film. Eqn (3) calculates the modified incident photon distribution on the cell surface ($\phi_{LDS}(\lambda)$), where $\phi(\lambda)$ is the incident photon distribution of AM1.5G sunlight. The calculation results from eqn (1)–(3) are depicted in Fig. 4.

It is noted in Fig. 4a that placing an LDS film of **Perylene-TPE** on the surface of a CdTe solar cell will directly increase its output J_{sc}. The enhancement in J_{sc} ($J_{LDS}\%$) exhibits a faster increase phase when the concentration of **Perylene-TPE** is below 1.0%, but a slower increase phase when the concentration is beyond 1.0%, and finally reaches a plateau with a maximum at 2.95% of $J_{LDS}\%$ at 2.0% of **Perylene-TPE** concentration. The increasing pattern of $J_{LDS}\%$ along with **Perylene-TPE** concentration in the LDS film can be explained by the Beer–Lambert law that the percentage of the incident light transmission exhibits exponential decay with the increase of the molecular concentration. In Fig. 4b, the predicted results on the cell EQE reveal that the increase in J_{sc} is attributed to the enhancement of spectral response of the CdTe solar cell below 500 nm. It is noted that the spectral response of the CdTe solar cell below 500 nm is gradually enhanced with the increase of **Perylene-TPE** concentration in the LDS film. The incident photon conversion efficiency of the CdTe solar cell at 400 nm is significantly increased by 41% from 0.44 to 0.62, which means more photons at 400 nm are absorbed and utilized by the CdTe solar cell. Since the LDS film does not affect the internal structure of the CdTe solar cell, such EQE enhancement in short-wavelength is solely from the modification of incident photon distribution by the LDS film. In Fig. 4c, it is revealed that with the increase of **Perylene-TPE**
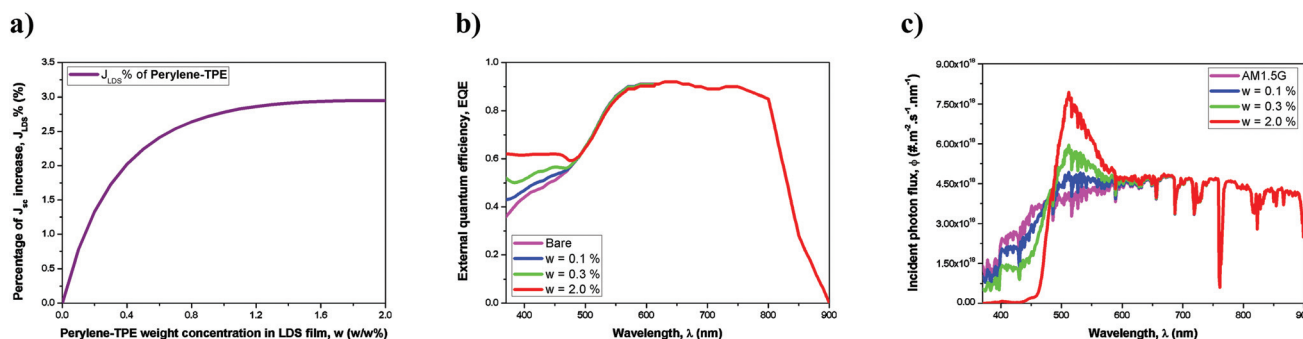

Fig. 4 Effects of **Perylene-TPE**-contained LDS films on (a) percentage of cell J_{sc} increase, (b) cell EQE, and (c) incident photon distribution (ϕ) on the cell surface.

This journal is © The Royal Society of Chemistry and Owner Societies 2015

Photochem. Photobiol. Sci., 2015, **14**, 833–841 | **837**

Paper

concentration, the number of photons below 500 nm is gradually decreased while the number of photons over 500 nm is gradually increased. Such a wavelength-shifting effect of the LDS film is achieved by the absorption and emission processes of **Perylene-TPE**.

Based on the results of the theoretical predictions by the LDS model, **Perylene-TPE** is able to enhance the output J_{sc} of a CdTe solar by up to 2.95%. Therefore, further investigations on the LDS capabilities of the LDS films of **Perylene-TPE** were carried out on a small lab-made CdTe solar cell.[37] LDS films were prepared by doping **Perylene-TPE** into PMMA. The concentration was varied from 0 to 1.6%. In the experiment, index matching fluid was used to fill the interface between the LDS film and the front surface of the CdTe solar cell to reduce the refractive photon loss. J_{LDS}% values were obtained by measuring the output currents of the CdTe solar cell with and without the LDS film on its surface using a multimeter. A LDS film of **Perylene-TPE** and the CdTe solar cell used in the experiment, as well as the experimental results of J_{LDS}% along with the **Perylene-TPE** concentration are depicted in Fig. 5.

It is noted in Fig. 5a that the LDS film of **Perylene-TPE** is very thin and bendable. The color is yellow and translucent. Under the illumination by UV light, the film exhibits greenish-blue (cyan) fluorescence. The color is consistent with the observed emission spectrum centered at 512 nm in Fig. 1. The size of the LDS film is the same as the surface area of the CdTe

solar cell. Placing the LDS film on the surface of a CdTe solar cell does not change its appearance under normal light but exhibits cyan fluorescence on its surface under UV illumination. In Fig. 5b, the increasing pattern of J_{LDS}% with the increase of **Perylene-TPE** concentration is consistent with the theoretical prediction in Fig. 4a. The error bars in Fig. 5b are due to the slight variation of fluorophore concentration during the preparation of the LDS films. The maximum of J_{LDS}% is found around 3.30 ± 0.31%, which is close to the theoretically predicted value of 2.95%. Further I–V measurements show that the short circuit current (I_{sc}) of the CdTe solar cell was increased by 3.42% with a 0.12% increase in its open circuit voltage (V_{oc}) but a 2.21% decrease in its fill factor (FF), which resulted in the power conversion efficiency of the CdTe solar cell being increased from 5.68% to 5.75% by only 1.26% (Table S2†). Since LDS is not expected to affect V_{oc} and FF theoretically, the increase in V_{oc} and decrease in FF may come from the effect of the index matching fluid used in our experiment. The J_{LDS}% difference between the theoretically predicted value and the two experimental values is due to two possible uncertainties of our measurements. One is because the calibration of the incident light from the solar simulator is obtained using a solar power meter rather than a calibrated solar cell. The other is because the J_{LDS}% value of 3.30 ± 0.31% is obtained using a multimeter while 3.42% is obtained using a sourcemeter. However, no matter what kind of devices were used to obtain J_{LDS}%, 3.30% ± 0.31% of J_{sc} enhancement by **Perylene-TPE** is comparable to the current commercially available LDS material – Y083 (3.28% ± 0.37%) in a most recent report, suggesting that **Perylene-TPE** is a good candidate for substituting Y083.[38]

Conclusion

In conclusion, in this work, a CN-free hydrocarbon fluorophore (**Perylene-TPE**) was synthesized as a new luminescent down-shifting (LDS) material. Its photophysical properties in both solution state and solid state were studied. The unity fluorescence quantum yield of **Perylene-TPE** that was observed in its solid state is believed to be from its characteristics of intramolecular energy transfer (IET) and restricted internal rotation (RIR). Its IET characteristic was investigated by quantum chemical calculations, with the conclusion drawn that the energy transfers from its TPE group to its perylene group, and that its perylene group dominates the electron transition of **Perylene-TPE** during its absorption and emission processes. Its RIR characteristic was examined by measuring the fluorescence quantum yields of **Perylene-TPE** in water–acetonitrile mixtures with various water fractions, concluding that the non-radiative decay rate is significantly decreased by restricting the internal σ-bond rotation. For the photovoltaic application of **Perylene-TPE**, a theoretical model was proposed to examine its LDS capability, suggesting that the LDS film of **Perylene-TPE** may increase the output short circuit current density (J_{sc}) of a CdTe solar cell by 2.95%, enhance the spectral response of
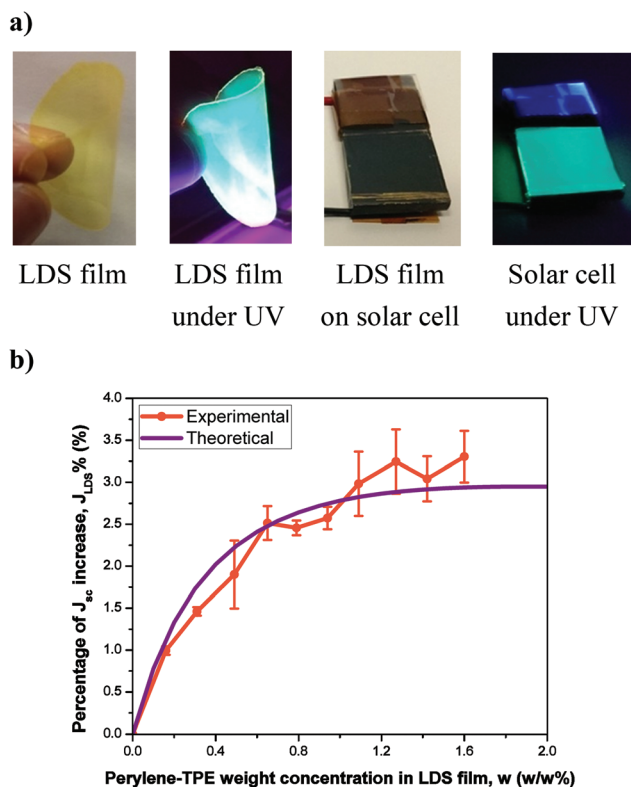
a)

| LDS film | LDS film under UV | LDS film on solar cell | Solar cell under UV |

b)

Fig. 5 Pictures of (a) a LDS film of **Perylene-TPE** and the CdTe solar cell used in the experiment, and (b) the experimental results of J_{LDS}% along with the **Perylene-TPE** concentration.

a CdTe solar cell at 400 nm by 41%, and shift the incident solar photon distribution from short-wavelength (<500 nm) to long-wavelength (>500 nm). Experimentally, placing an LDS film of **Perylene-TPE** on a CdTe solar cell can enhance its output J_{sc} by as high as 3.30 ± 0.31%, which is comparable to the current commercially available LDS material – Y083 (3.28% ± 0.37%).

Experimental

Spectroscopic measurements

Absorption spectra were recorded using a Beckman Coulter DU730 Life Science UV-Vis spectrophotometer at room temperature. Emission spectra were collected on an ISS PC1 photon counting spectrofluorometer at room temperature. Fluorescence lifetimes were measured on a HORIBA JOBIN YVON fluorocube.

The fluorescence lifetime data were fitted by a single-exponential equation:

$$I(t) = \alpha \cdot e^{-\frac{t}{\tau_f}}$$

Theoretical calculations

Theoretical calculations were conducted using the Gaussian 09 package. Ground state (S_0) geometry was optimized by using the DFT B3LYP/6-31G(d) function. HOMO and LUMO as well as the corresponding energy and charge distribution were then calculated based on the optimal geometry.

LDS film preparation

Briefly, 7.5 g of PMMA powder (purchased from TCI America) was dissolved in 100 g of toluene in a 250 mL flask. The mixture was stirred overnight and the insoluble PMMA was filtered off. Then, 1.8 g of the PMMA solution was finely mixed with a variable amount of the synthesized fluorophore in a 10 mL vial. The fluorophore–PMMA mixture was poured into a Petri dish (R25 × 15 mm). The films were finally cut and peeled off from the Petri dish in warm water. This preparation method can yield films with the thickness of about 50 μm.

LDS theoretical model

The expressions of the factors and J_{loss}% are:

$$F_{abs} = \frac{\int [1 - T(\lambda)]\phi(\lambda)d\lambda}{\int \phi(\lambda)d\lambda}$$

$$F_{em} = \frac{\int EQE(\lambda)Em(\lambda)d\lambda}{\int Em(\lambda)d\lambda}$$

$$F_{pc} = \Phi_f \times \eta_{opt}$$

$$F_{cell} = \frac{\int EQE(\lambda)\phi(\lambda)d\lambda}{\int \phi(\lambda)d\lambda}$$

$$J_{loss}\% = \frac{\int EQE(\lambda)[1 - T(\lambda)]\phi(\lambda)d\lambda}{\int EQE(\lambda)\phi(\lambda)d\lambda}$$

In the expression F_{abs}, $T(\lambda)$ is the transmission of the LDS film. Its value can be calculated by the molar concentration (c, mol L^{-1}) of **Perylene-TPE** according to the Beer–Lambert law:

$$T(\lambda) = 10^{-Abs(\lambda)} = 10^{-\varepsilon(\lambda) \cdot l \cdot c}$$

where $\varepsilon(\lambda)$ is the wavelength-dependent absorption coefficient (M^{-1} cm^{-1}), l is the thickness of the LDS film (cm).

c can be calculated by the weight concentration (w) if the density of the LDS film ($\rho = 1.2$ g cm^{-3}) and molecular weight of **Perylene-TPE** ($M_W = 583$ g mol^{-1}) are known:

$$c = w\frac{\rho}{M_w}$$

In the expression of F_{em}, $Em(\lambda)$ is the emission spectrum of the LDS film, which is the same as the emission spectrum of **Perylene-TPE** in PMMA the solid film in Fig. 1.

In the expression of F_{pc}, Φ_f is the solid state fluorescence quantum yield of the LDS film, which is equal to the fluorescence quantum yield of **Perylene-TPE** in the PMMA solid film in Table 1. η_{opt} is the optical efficiency of the LDS film, which is 82.3% considering 12.7% of the photon surface loss and 5% of the photon side loss that are theoretically calculated from the refractive index of the PMMA and the size of the LDS film.[1]

Photovoltaic measurements

The CdTe solar cell was manufactured by a magnetron sputtering method and was provided by Professor Alvin Compaan, University of Toledo.[37] The structure of the CdTe solar cell is glass/SnO$_2$:F/CdS/CdTe/Cu/Au. The thickness of the CdS buffer layer is 70–80 nm. The dimensions of the CdTe solar cell are 15 mm × 15 mm × 3 mm and its active area is 0.5 cm^2. A 150 W solar simulator (model# 96000, Newport Corporation) equipped with a xenon lamp and an AM1.5G filter (model# 81092, Newport Corporation) was used as the light source. The incident power density was 100 mW cm^{-2}, measured by using a solar power meter (Amprobe SOLAR-100). Photocurrent (I_{ph}) was measured directly by using a digital multimeter (GB electrical GDT200A). Photovoltaic parameters including I_{sc}, V_{oc}, FF and η_{eff} were obtained by using a Keithley 2420 3A sourcemeter. Index matching fluid (mode# F-IMF-105, Newport Corporation, 1.52@589 nm) was used to fill the interface between the LDS film and the front surface of the CdTe solar cell to reduce the refractive photon loss. J_{LDS}% is calculated by:

$$J_{LDS}\% = \left(\frac{I_{ph,cell+LDS}}{I_{ph,cell}} - 1\right) \times 100\%$$

Acknowledgements

This journal is © The Royal Society of Chemistry and Owner Societies 2015

Photochem. Photobiol. Sci., 2015, **14**, 833–841 | **839**

References

1 E. Klampaftis, D. Ross, K. R. McIntosh and B. S. Richards, Enhancing the performance of solar cells via luminescent down-shifting of the incident spectrum: A review, *Sol. Energy Mater. Sol. Cells*, 2009, **93**, 1182.

2 B. M. van der Ende, L. Aarts and A. Meijerink, Lanthanide ions as spectral converters for solar cells, *Phys. Chem. Chem. Phys.*, 2009, **11**, 11081.

3 X. Huang, S. Han, W. Huang and X. Liu, Enhancing solar cell efficiency: the search for luminescent materials as spectral converters, *Chem. Soc. Rev.*, 2013, **42**, 173.

4 W. G. J. H. M. v. Sark, A. Meijerink, R. E. I. Schropp, J. A. M. v. Roosmalen and E. H. Lysen, Modeling improvement of spectral response of solar cells by deployment of spectral converters containing semiconductor nanocrystals, *Semiconductors*, 2004, **38**, 962.

5 V. Svrcek, A. Slaoui and J.-C. Muller, Silicon nanocrystals as light converter for solar cells, *Thin Solid Films*, 2004, **451–452**, 384.

6 T. Maruyama and R. Kitamura, Transformations of the wavelength of the light incident upon solar cells, *Sol. Energy Mater. Sol. Cells*, 2001, **69**, 207.

7 B. S. Richards and K. R. McIntosh, Overcoming the poor short wavelength spectral response of CdS/CdTe photovoltaic modules via luminescence down-shifting: ray-tracing simulations, *Prog. Photovoltaics: Res. Appl.*, 2007, **15**, 27.

8 T. Jin, S. Inoue, S. Tsutsumi, K.-i. Machida and G.-y. Adachi, High conversion efficiency photovoltaic cell enhanced by lanthanide complex phosphor film coating, *Chem. Lett.*, 1997, **27**, 171.

9 O. Moudam, B. C. Rowan, M. Alamiry, P. Richardson, B. S. Richards, A. C. Jones and N. Robertson, Europium complexes with high total photoluminescence quantum yields in solution and in PMMA, *Chem. Commun.*, 2009, 6649.

10 Y. Li and W.-J. Dong, Theoretical modeling on luminescent down-shifting process: A Discussion on luminescent molecule design, *Photovoltaic Specialist Conference (PVSC), 2014 IEEE 40th*, 2014, p. 2243.

11 I. B. Berlman, Empirical correlation between nuclear conformation and certain fluorescence and absorption characteristics of aromatic compounds, *J. Phys. Chem.*, 1970, **74**, 3085.

12 N. I. Nijegorodov and W. S. Downey, The influence of planarity and rigidity on the absorption and fluorescence parameters and intersystem crossing rate constant in aromatic molecules, *J. Phys. Chem.*, 1994, **98**, 5639.

13 L. H. Slooff, R. Kinderman, A. R. Burgers, N. J. Bakker, J. A. M. van Roosmalen, A. Buchtemann, R. Danz and M. Schleusener, Efficiency enhancement of solar cells by application of a polymer coating containing a luminescent dye, *J. Sol. Energy Eng.*, 2007, **129**, 272.

14 F. Galluzzi and E. Scafe, Spectrum shifting of sunlight by luminescent sheets: performance evaluation of photovoltaic applications, *Sol. Energy*, 1984, **33**, 501.

15 A. F. Mansour, On enhancing the efficiency of solar cells and extending their performance life, *Polym. Test.*, 2003, **22**, 491.

16 L. Danos, T. Parel, T. Markvart, V. Barrioz, W. S. M. Brooks and S. J. C. Irvine, Increased efficiencies on CdTe solar cells via luminescence down-shifting with excitation energy transfer between dyes, *Sol. Energy Mater. Sol. Cells*, 2012, **98**, 486.

17 D. Ross, E. Klampaftis, J. Fritsche, M. Bauer and B. S. Richards, Increased short-circuit current density of production line CdTe mini-module through luminescent down-shifting, *Sol. Energy Mater. Sol. Cells*, 2012, **103**, 11.

18 D. Ross, D. Alonso-Alvarez, E. Klampaftis, J. Fritsche, M. Bauer, M. G. Debije, R. M. Fifield and B. S. Richards, The impact of luminescent down shifting on the performance of CdTe photovoltaics: impact of the module vintage, *IEEE J. Photovoltaics*, 2014, **4**, 457.

19 E. Klampaftis, D. Ross, S. Seyrling, A. N. Tiwari and B. S. Richards, Increase in short-wavelength response of encapsulated CIGS devices by doping the encapsulation layer with luminescent material, *Sol. Energy Mater. Sol. Cells*, 2012, **101**, 62.

20 Y. Li, Z. Li, Y. Wang, A. Compaan, T. Ren and W.-J. Dong, Increasing the power output of a CdTe solar cell via luminescent down shifting molecules with intramolecular charge transfer and aggregation-induced emission characteristics, *Energy Environ. Sci.*, 2013, **6**, 2907.

21 R. P. Schwarzenbach, P. M. Gschwend and D. M. Imboden, *Environmental Organic Chemistry*, John Wiley & Sons, NJ, USA, 2nd edn, 2005.

22 A. Surleva, R. Gradinaru and G. Drochioiu, Cyanide poisoning: from physiology to forensic analytical chemistry, *Int. J. Crim. Invest.*, 2012, **2**, 79.

23 Environmental impacts of perylene: http://www.nature.nps.gov/hazardssafety/toxic/perylene.pdf (accessed 9.5.2014).

24 MSDS of tetraphenylethylene: http://images.mpbio.com/docs/msds/aust/en/219212-EN-AUST.pdf (accessed 9.5.2014).

25 V. K. Ahluwalia, *Green Solvents For Organic Synthesis*, Alpha Science International Ltd, 2009.

26 A. R. Karikachery, H. B. Lee, M. Masjedi, A. Ross, M. A. Moody, X. Cai, M. Chui, C. D. Hoff and P. R. Sharp, High quantum yield molecular bromine photoelimination from mononuclear platinum(IV) complexes, *Inorg. Chem.*, 2013, **52**, 4113.

27 Y. Avlasevich and K. Mullen, An efficient synthesis of quaterrylenedicarboximide NIR dyes, *J. Org. Chem.*, 2007, **72**, 10243.

28 Y. Hong, S. Chen, C. W. Leung, J. W. Lam, J. Liu, N. W. Tseng, R. T. Kwok, Y. Yu, Z. Wang and B. Z. Tang, Fluorogenic Zn(II) and chromogenic Fe(II) sensors based on terpyridine-substituted tetraphenylethenes with aggregation-induced emission characteristics, *ACS Appl. Mater. Interfaces*, 2011, **3**, 3411.

29 A guide to recording fluorescence quantum yields: http://www.horiba.com/fileadmin/uploads/Scientific/Documents/Fluorescence/quantumyieldstrad.pdf (accessed 1.24.2015).

30 L.-O. Pålsson and A. P. Monkman, Measurements of solid-state photoluminescence quantum yields of films using a fluorimeter, *Adv. Mater.*, 2002, **14**, 757.

31 J. R. Lakowicz, *Principles of Fluorescence Spectroscopy*, Springer Science+Business Media, NY, USA, 3rd edn, 2006.

32 W. Z. Yuan, P. Lu, S. Chen, J. W. Lam, Z. Wang, Y. Liu, H. S. Kwok, Y. Ma and B. Z. Tang, Changing the behavior of chromophores from aggregation-caused quenching to aggregation-induced emission: development of highly efficient light emitters in the solid state, *Adv. Mater.*, 2010, **22**, 2159.

33 Y. Hong, J. W. Lam and B. Z. Tang, Aggregation-induced emission: phenomenon, mechanism and applications, *Chem. Commun.*, 2009, 4332.

34 Y. Hong, J. W. Lam and B. Z. Tang, Aggregation-induced emission, *Chem. Soc. Rev.*, 2011, **40**, 5361.

35 Y. Li, T. Ren and W.-J. Dong, Tuning photophysical properties of triphenylamine and aromatic cyano conjugate-based wavelength-shifting compounds by manipulating intramolecular charge transfer strength, *J. Photochem. Photobiol., A*, 2013, **251**, 1.

36 Y. Li, L. Scudiero, T. Ren and W.-J. Dong, Synthesis and characterizations of benzothiadiazole-based fluorophores as potential wavelength-shifting materials, *J. Photochem. Photobiol., A*, 2012, **231**, 51.

37 A. Gupta and A. D. Compaan, All-sputtered 14% CdS/CdTe thin-film solar cell with ZnO : Al transparent conducting oxide, *Appl. Phys. Lett.*, 2004, **85**, 684.

38 Y. Li, Z. Li, T. Ablekim, T. Ren and W.-J. Dong, Rational design of tetraphenylethylene-based luminescent down-shifting molecules: photophysical studies and photovoltaic applications in a CdTe solar cell from small to large units, *Phys. Chem. Chem. Phys.*, 2014, **16**, 26193.